

Synthesis and Characterization of Serial Random and Block-Copolymers Based on Lactide and Glycolide¹

Zongrui Zhang^{a,b}, Xinyu Wang^{a,b,*}, Rong Zhu^{a,b}, Yiyu Wang^{a,b},
Binbin Li^{a,b}, Yanxu Ma^b, and Yixia Yin^{a,b}

^aState Key Laboratory of Advanced Technology for Materials Synthesis and Processing,
Wuhan University of Technology, Wuhan 430070, China

^bBiomedical Materials and Engineering Research Center of Hubei Province,
Wuhan University of Technology, Wuhan, 430070 China

*e-mail: wangxinyu@whut.edu.cn

Received April 28, 2016;

Revised Manuscript Received June 7, 2016

Abstract— The objective of this study is to investigate the properties of poly(lactide-*co*-glycolide) with different composition ratios and PLGA-PEG-PLGA copolymers synthesized by ring-opening polymerization method. Their compositions, crystallization properties, thermal and degradation behaviors, hydrophilicity and biocompatibility were studied. Our results demonstrate that poly(lactide-*co*-glycolide) with a 90% lactide and PLGA-PEG-PLGA show some crystallization properties. While as the decrease of lactide content in polymers, poly(lactide-*co*-glycolide) become amorphous, whereas, their hydrophilicity have been improved on the contrary. Compared to poly(lactide-*co*-glycolide), the PLGA-PEG-PLGA copolymer has a better hydrophilicity for the existence of polyethylene glycol block. Furthermore, both these polymers display easy controlled degradation properties and good cell compatibility.

DOI: 10.1134/S1560090416060191

INTRODUCTION

Recently, the research of the synthetic biodegradable polymers have attracted a strong interest, in which the biomedical aliphatic copolyesters have been proved to be promising materials in tissue engineering and drug delivery system (DDS). As an aliphatic polyester, poly(lactide-*co*-glycolide) (PLGA) polymers were composed of lactide (LA) and glycolide (GA) monomers [1]. The synthesis of PLGA was carried out via two methods: direct melting polymerization resulting in polymers of low molecular weight (MW) and ring-opening polymerization resulting in high MW product as well as better mechanical properties in general [2, 3]. In the past two decades, PLGA has been extensively studied in many fields including fracture fixation [4], tissue repair engineering [5], surgical suture [6], artificial organs [7, 8] and DDS [9] owing to desirable properties such as good biocompatibility, alterable biodegradation rates and technical versatility.

As we know, the main factors influencing polymer degradation behavior are chemical structure, crystallinity, MW and molecular mass distribution [10, 11]. As Wu [12] has reported, PLGA with a higher MW, degrades faster than with lower MW, besides PLGA degrades more rapidly when containing higher GA

content. Vey et al. [13] have studied PLGA (LA/GA mole ratio = 50/50 and 75/25) by considering that their degradation rates are coordinated with the tissue growth rate. Furthermore, PLGA with these two ratios are the most commonly used carriers in controlled DDS [14, 15]. In order to obtain controlled release of encapsulated therapeutics from PLGA polymers, their compositions, size and surface properties can be customized to achieve different loadings and distinct polymer erosion profiles [16, 17]. Greater attention has been directed to the importance of particle shape and morphology for improved DDS applications [18]. Di [19] has developed a novel Laser-generated-focused ultrasound (LGFU)-responsive drug-loaded PLGA nanoparticles to precisely control the release of therapeutics in a spatiotemporal manner and potentially suppress detrimental effects to the surrounding tissues. Furthermore, a docetaxel-loaded PLGA-TPGS/Poloxamer 235 nanoparticles system has been produced to overcome multidrug resistance, which has considerable therapeutic potential for breast cancer [20]. Nevertheless, PLGA has some shortcomings of poor surface wettability and cellular affinity, which limits its applications and only enables it to deliver hydrophobic drugs.

PLGA-PEG-PLGA copolymers composed of PLGA and polyethylene glycol (PEG) are gaining

¹ The article is published in the original.

attentions in controlled DDS because of their good thermo-responsive and biocompatibility [21]. Chen [22] has confirmed that the thermo-sensitive and biodegradable PLGA-PEG-PLGA hydrogel holds potential as a barrier device to decrease peridural scarring and achieves sustained release of drugs from the hydrogel matrix. In addition, the injectable PLGA-PEG-PLGA thermogel has been revealed a biocompatible carrier for sustained delivery of bioactive agents into the eyes [23]. PLGA-PEG-PLGA copolymer degraded by hydrolysis and the rate depended on its MW, the LA/GA ratios and the PEG content [24–26]. The existence of hydrophilic PEG block will greatly improve PLGA-PEG-PLGA hydrophilicity, which enables it to deliver both hydrophobic and hydrophilic drugs [27, 28]. Song [29] has researched the in vitro release of docetaxel in PLGA-PEG-PLGA carrier, which showed prolonged exposure and better inhibitory on tumor growth. Also, Xu [30] has designed the siRNA-encapsulating PEG-*Dlink_m*-PLGA nanoparticle which gained efficiently prolonged circulation in the blood and preferential accumulation in tumor sites via the PEGylation. As a consequence, PLGA-PEG-PLGA copolymer is an ideal candidate for pharmaceutical applications [31] insolubilization and stabilization peptides and protein drugs, such as vascular endothelial growth factor [32], insulin [33] and calcitonin [34].

As PLGA and PLGA-PEG-PLGA copolymers have these outstanding applications for DDS, more attentions must be dedicated to investigate the characteristics of these two polymers putting special emphasis on the differences on physico-chemical properties. Currently, a series of PLGA with different compositions and PLGA-PEG-PLGA copolymers were systematically synthesized and researched. These prepared materials were confirmed as PLGA and PLGA-PEG-PLGA from IR analysis. The effect of the PEGylation on some properties including crystallization behavior, thermal properties, hydrophilicity and biocompatibility have been studied in detail. Therefore, the appropriate copolymers with good cellular affinity and sustained controlled degradation rate were explored to prepare drug-loaded microspheres through this experiment results.

EXPERIMENTAL

Materials

The experimental materials LA and GA were supplied by Huawei biological technology co, LTD (Wuhan, CHN). The stannous octoate, lauryl alcohol and PEG (2000) were obtained from Huashun biological technology co, LTD (Wuhan, CHN). Chloroform, toluene, tetrahydrofuran (THF), tetramethylsilane (TMS), diethyl ether and methanol were all purchased from Shenshi chemical instrument co, LTD (Wuhan, CHN). Also the tetrazolium dye 3-(4,5-

dimethylthiazol-2-yl)-2, 5-diphenyltetrazolium bromide (MTT) and human neuroglioma (U251) were obtained from Sigma. These above analytical grade solvents must be fully dried by adding molecular sieve before using.

Synthesis of PLGA and PLGA-PEG-PLGA Copolymers

PLGA were synthesized based on ring-opening polymerization technique. Before polymerization, two raw LA and GA monomers were recrystallized four times and dried in vacuum oven for 72 h. Then, LA and GA with a molar ratio of 50/50 were placed in an ampoule, which already contained solutions of stannous octoate (0.02% m/v) and lauryl alcohol (0.01% m/v). Afterwards, the ampoule was sealed after degassing (about 80 Pa) and imbedded in a silicone oil bath at 140°C for 24h. For the synthesis of PLGA-PEG-PLGA, PEG (5 g) and 100 mL of toluene were placed in the round-bottom flask. After dehydration for 24 h, the same mole amount of LA and GA were added into the flask, which afterwards was heated at 150°C for 5 h to mix uniformity. The reaction was started by adding two droplets of stannous octoate and it lasted for 12 h. After the synthesis, PLGA and PLGA-PEG-PLGA were dissolved in chloroform, precipitated in excess of anhydrous methanol and refrigerant diethyl ether respectively for further measurements. Both of them were stored in a vacuum desiccator after dried in vacuum oven at 40°C for 48 h. Later on, PLGA-PEG-PLGA (75/25) with LA/GA molar ratio of 75/25 and PLGA of 60/40, 70/30, 80/20, and 90/10 molar ratio of LA/GA were prepared by the aforementioned procedures (Table 1). All these materials were dissolved in chloroform and dried in room temperature to make films for the FTIR, XRD, hydrophilicity and degradation tests.

Characterization

The chemical structure analysis was performed by FTIR spectroscopy (Thermo electron, USA). The infrared absorption spectra were detected over a range of 4000–500 cm^{-1} by using 64 scans with a resolution of 4 cm^{-1} at 25°C. The XRD (Bruker D8 Advance, Germany) measurements were used to ascertain polymers' crystallization with a $\text{CuK}\alpha$ radiation (Ni filter) and a diffraction 2θ range of 5°–50° (the polymer films used in FTIR and XRD tests were presented in synthesis part). The GPC (Agilent, America) was employed to determine MWD. The collected totally dried polymers were dissolved in THF about 3 mg/mL at room temperature, taking THF as the eluent with a flow rate of 1.0 mL/min and regarding monodisperse polystyrene distribution curve as a universal calibration parameter. In order to calculate polymer compositions, ^1H NMR Bruker AVANCE 500MHZ (AV 500) spectrometer at room temperature were performed, taking CDCl_3 as eluent and TMS as internal reference.

Table 1. The characteristics of synthesized PLGA and PLGA-PEG-PLGA

| Sample | Feed monomer ratios, mole | | | Compositions (LA/GA/PEG) ^a , mole | | | Molecular weight characteristics ^b | |
|---------------|---------------------------|----|-----|--|------|------|---|------|
| | LA | GA | PEG | LA | GA | PEG | $M_n \times 10^{-3}$ | PDI |
| PLGA | 50 | 50 | 0 | 49.7 | 50.3 | 0 | 51.3 | 1.25 |
| PLGA | 60 | 40 | 0 | 61.3 | 38.7 | 0 | 59.5 | 1.21 |
| PLGA | 70 | 30 | 0 | 71.7 | 28.3 | 0 | 66.0 | 1.17 |
| PLGA | 80 | 20 | 0 | 80.8 | 19.2 | 0 | 70.6 | 1.18 |
| PLGA | 90 | 10 | 0 | 90.2 | 9.8 | 0 | 68.6 | 1.19 |
| PLGA-PEG-PLGA | 40 | 40 | 20 | 41.9 | 40.0 | 18.1 | 9.1 | 1.26 |
| PLGA-PEG-PLGA | 60 | 20 | 20 | 62.6 | 19.7 | 17.7 | 9.4 | 1.20 |

^aThe data were calculated from ¹H NMR measurements.

^bThe data were obtained from GPC analysis.

The DSC (PE, USA) and TG (NETZACH, Germany) were conducted under nitrogen atmosphere, at a constant heating rate of 10 grad/min in the temperature range from -100 to 100°C and 25 to 400°C respectively.

The polymer hydrophilicity was measured using contact angle goniometer (OCA-35, Data physics, Germany). The contact angle size was tested as soon as the testing liquid was dropped on the films using a micro-syringe. Each sample's average value was obtained from at least 3 measurements with 0.5 cm testing liquid intervals. PLGA polymer degradation properties were obtained by immersing polymer films into PBS (pH = 7.4) in screw-capped tubes which then were placed horizontally in an orbital shaker (HZQ-F160, Harbin, China) maintained at 37°C. At preselected time intervals, we measured the solutions' pH values, afterwards, removing the supernatant, adding 8 mL of fresh medium and placing these tubes back in the shaker. In order to study PLGA and PLGA-PEG-PLGA biocompatibility, the exponential growth phase U251 cells were seeded in 96-well plates (3×10^4 per well) in DMEM medium containing 10% fetal bovine serum, supplemented with 1% penicillin and streptomycin. Polymer cytotoxicity was assessed by MTT assay after appropriate dilution in culture medium, for 24, 48, 72 h, respectively. Each data was obtained by averaging six measurements per sample, and represented as means \pm standard deviation.

RESULTS AND DISCUSSION

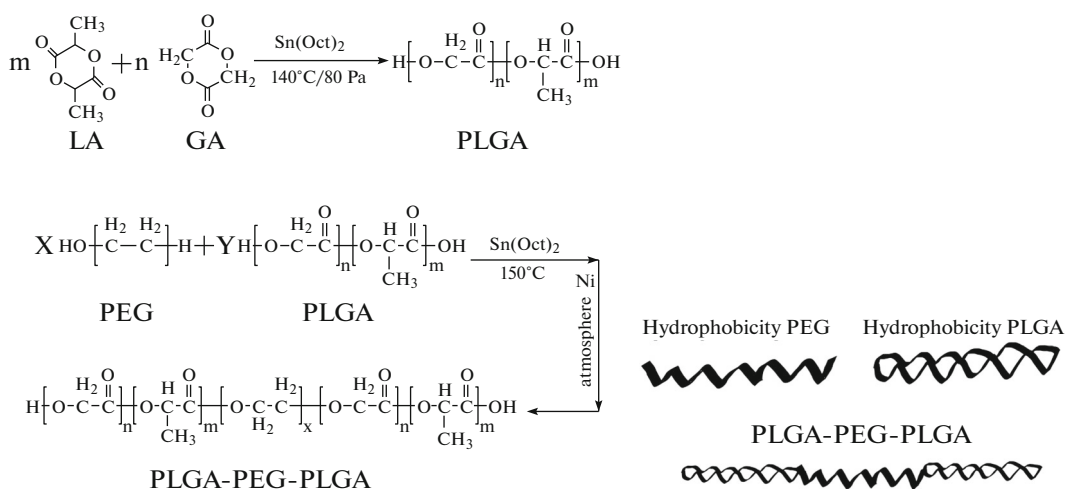
Copolymers Synthesis and Characterization

The preparation process of PLGA and PLGA-PEG-PLGA is presented in Scheme 1. In order to synthesize PLGA polymers with higher MW a few experimental parameters and details should be controlled. Firstly, before sealing the ampoules, they were connected to a high vacuum pump monitored using an electronic vacuum gauge to remove the solvent. In our

experiments, the vacuum in the ampoules reached 80 Pa. What is more, the ampoules should be hand shaken continuously until the LA and GA crystals are completely melted in the oil bath (140°C) to assure an even distribution of the catalyst. As Wang [35] has reported, by controlling the vacuum degree, the polymerization parameters especially the residual water content can be controlled to assure the reproducibility of the MW. Thereafter, a series of PLGA and PLGA-PEG-PLGA (50/50), (75/25) were synthesized while the reaction parameters were fixed. Since the reactivity ratios of LA and GA were different, the synthetic products were random copolymers.

The IR spectra (Fig. 1a) illustrate all characteristic groups for LA, GA and PLGA. An intense band at 1760 cm^{-1} due to the stretch of carbonyl groups is found in all three spectra. Moreover, the stretching bands of C-H groups in the region between 2950 and 3000 cm^{-1} are observed. The absorption band at 3510 cm^{-1} is attributed to PLGA terminal hydroxyl group. The 1420 and 1320 cm^{-1} bands, which can only be found in polymer spectrum, are assigned to the bending vibration bands of CH_2 and CH (CH_3). The disappearing of β -glycolide characteristic band at 1310 cm^{-1} in PLGA spectrum proves the ring-opening reaction indeed occurred in LA and GA. Compared to LA and GA spectra, the absence of absorption bands between 935 and 864 cm^{-1} in polymer spectrum, characteristic of the ring C-H deformation vibration peak made clear proof of synthesized PLGA polymer.

For the PLGA-PEG-PLGA (50/50) copolymer IR spectrum is shown in Fig. 1b, the major bands assigned to the structure of PLGA-PEG-PLGA are observed at 3497 cm^{-1} (-OH), 2877 cm^{-1} (-OCH₂), 1757 cm^{-1} (C=O), 1455 and 1352 cm^{-1} (-CH₂), 1130 cm^{-1} (C-O). By comparing the PLGA-PEG-PLGA spectrum with that of PEG and PLGA, it is characteristic that the absorption band at 3497 cm^{-1} belongs to the hydroxyl stretching of LA or GA struc-



Scheme 1.

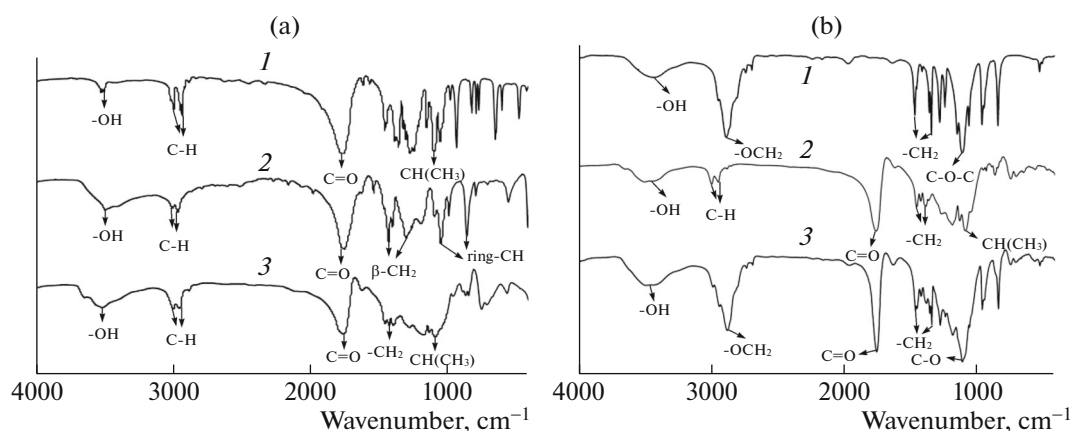


Fig. 1. FTIR spectra of (a) (1) lactide, (2) glycolide and (3) PLGA (50/50), (b) (1) PEG, (2) PLGA and (3) PLGA-PEG-PLGA (50/50) copolymers.

ture fragments in PLGA-PEG-PLGA. The bands at 1455 and 1352 cm^{-1} , both founded in PEG and PLGA spectra, are assigned to their methyl groups. The bands at 2877, 1130, and 1757 cm^{-1} are attributed to PLGA-PEG-PLGA methylene group near to oxygen atom, C–O bond and the stretching vibration of C=O respectively. So, it is confirmed that PEG ether linkage exists in triblock copolymer and the reaction between PLGA and PEG has been effective. Therefore, it can be concluded that PLGA-PEG-PLGA is successfully synthesized.

Figure 2 shows the ^1H NMR spectra of PLGA (50/50) and PLGA-PEG-PLGA (50/50) copolymers. The characteristic peaks are used to identify the characteristic functional groups (Table 2). The signals observed at 1.66 and 5.20 ppm may be referred to protons of methyl and methyne groups of LA monomer unit correspondingly; meanwhile, the signals at 4.99 and 3.64 ppm respectively can be ascribed to protons

of methylene group (CH_2) of GA and PEG [36–38]. As seen in Table 1, the copolymer composition is closed to the feed monomer ratios.

According to GPC data (Table 1), the polymers formed are characterized by relatively narrow MWD, which confirms formation of copolymers rather than the mixture of homopolymers [39].

The degradation behavior, mechanical properties, solubility and degradability of PLGA are all related to MW, microstructure and chemical composition of polymer. Many comprehensive studies have demonstrated the core-shell structure of PLGA-PEG-PLGA used in DDS can overcome the barriers of systemic drug delivery to tumors and potential side effects [30, 33, 40, 41]. The composition and MW of PLGA-PEG-PLGA copolymers greatly affect the surface charge and release properties of PEG-modified nanoparticles [42]. It is of great importance to study

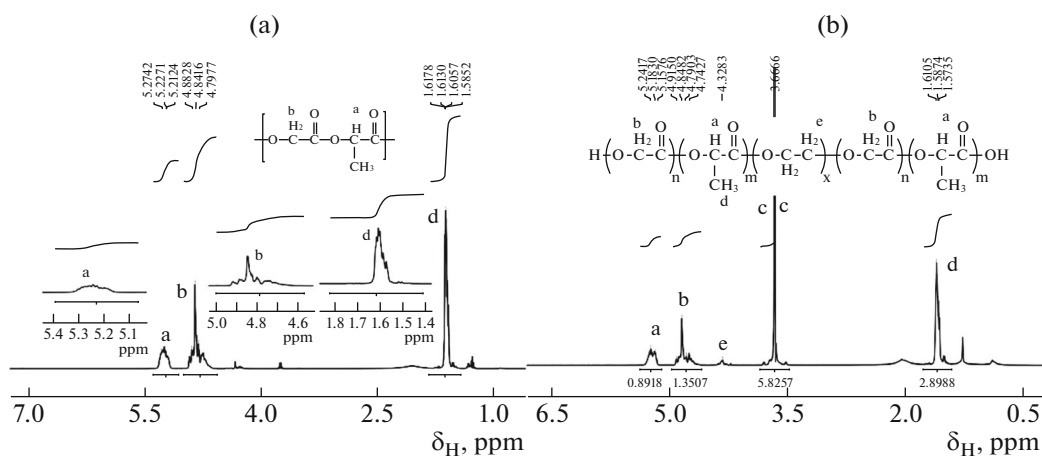


Fig. 2. ^1H NMR spectra of (a) PLGA (50/50), (b) PLGA-PEG-PLGA (50/50) copolymers.

what the direct influences do the different copolymer compositions have on their properties.

The crystallization properties of PLGA and PLGA-PEG-PLGA copolymers were determined by XRD. The XRD analysis results (Fig. 3a) show that there is no obvious prominent peaks in the patterns of PLGA polymers with LA molar ratio of 50–80%. However, the intense peak on PLGA (90 : 10) diffractogram at 14.44° indicates the presence of some crystallinity phase. The disordered-crystalline phase of PLGA is helpful for the sustained release of the encapsulated drugs.

As shown in Fig. 3b, the obvious prominent peaks appeared at 19.33° and 18.79° respectively in two PLGA-PEG-PLGA copolymer patterns suggest their crystalline nature. These changes in XRD patterns suggest partial conversions of PLGA from amorphous to crystalline state. Moreover, apart from the PLGA crystalline conversions, the presence of PEG block is another reason for the crystallinity changes in PLGA-PEG-PLGA. Probably, PEG acts as a lubricant between PLGA chains and causes strong chemical bonds between PEG and PLGA chain segments, which result in a better mechanical property of PLGA-PEG-PLGA for its crystalline structure. As a consequence, PLGA-PEG-PLGA with enhanced mechanical property will ensure the stability of both polymer matrices and loaded drugs which are very important in controlled DDS.

Compared with body temperature, the T_g determined polymers in a rubbery or glassy state plays an important role in the release of drugs from polymer matrices. A rubbery polymer has a higher permeability to water and loads more drugs than a glassy one, resulting in faster polymer hydration, degradation as well as drug release. However, polymer phases gradually convert from glassy state to rubbery state as its T_g decreases caused by hydration, which for a glassy poly-

mer results in a longer time lag for polymer degradation and drug release [43, 44].

The T_g of PLGA with different compositions was determined by DSC (Fig. 4a). PLGA polymers have T_g values varying from 27.7 to 46.2°C ; T_g increases with growth in LA content in PLGA.

To investigate the molecular level dispersion of PEG within the PLGA-PEG-PLGA copolymer, DSC thermograms were produced for pure PEG, PLGA (75/25), and PLGA-PEG-PLGA (75/25). As shown in Fig. 4b, PEG displayed an intense peak at 62.4°C is corresponding to its melting temperature according to the literatures [45, 46] and a drift in baseline corresponding to T_g at -35.2°C . The latter is close to T_g of PEG in PLGA-PEG-PLGA (-35.8°C). T_g of PLGA (31.2°C) is close to the value in block-copolymer (35.8°C).

PLGA with different compositions were subjected to TG analysis to investigate the influence of LA and GA ratios on their decomposition behavior by heating the samples from 25 to 400°C under nitrogen atmo-

Table 2. The ^1H NMR spectra data analysis of PLGA and PLGA-PEG-PLGA copolymers

| Number | Chemical shift δ_{H} , ppm | Corresponding proton |
|--------|--|--|
| 1(a) | 5.20 | CH of Lactide |
| 2(b) | 4.99 | CH_2 of Glycolide |
| 3(c) | 3.64 | CH_2 of PEG |
| 4(d) | 1.66 | CH_3 of Lactide |
| 5(e) | 4.30 | CH_2 of PEG between LA and GA |

a, b, c, d, e which represent the integral area of different chemical shifts were used to calculate the compositions of PLGA and PLGA-PEG-PLGA copolymers in the above equations 1 to 5.

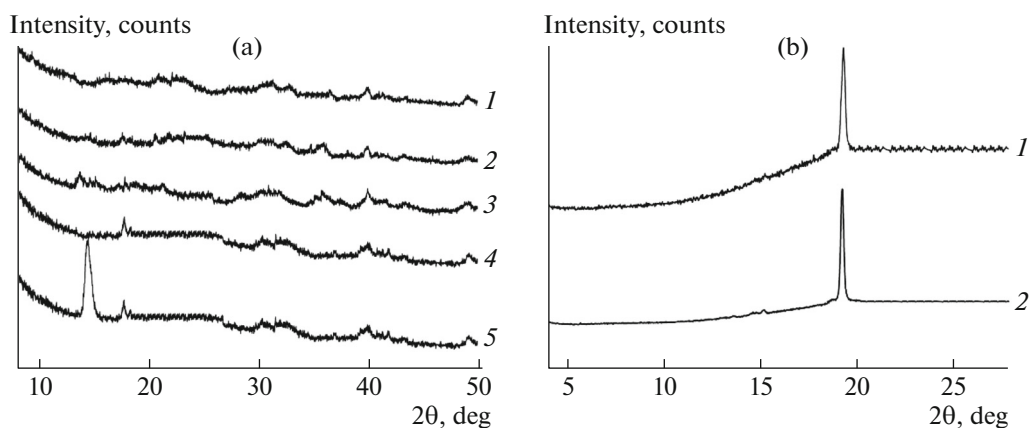


Fig. 3. X-ray diffraction patterns of (a) PLGA polymers with different LA/GA ratios: (1) 50/50, (2) 60/40, (3) 70/30, (4) 80/20, (5) 90/10; (b) (1) PLGA-PEG-PLGA (75/25) and (2) PLGA-PEG-PLGA (50/50) copolymers.

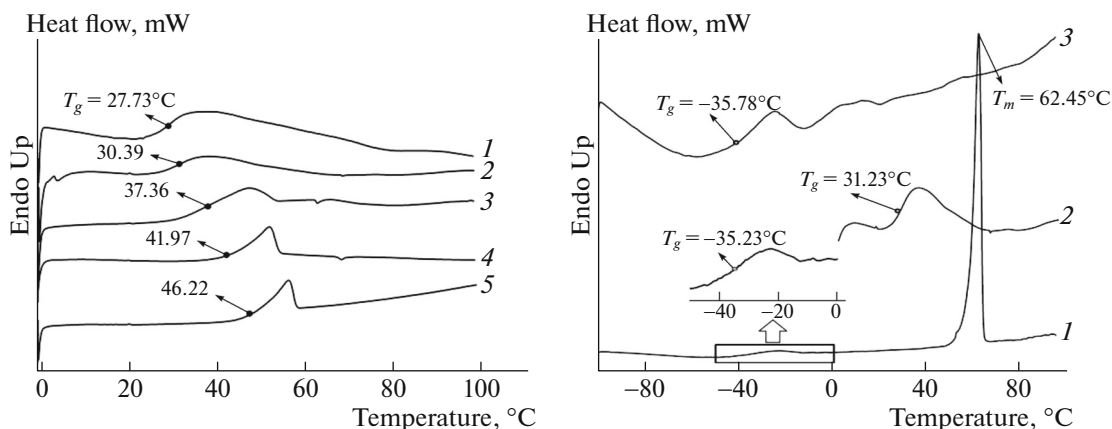


Fig. 4. The DSC curves of (a) PLGA polymers: (1) 50/50, (2) 60/40, (3) 70/30, (4) 80/20, (5) 90/10; (b) (1) PEG, (2) PLGA (75/25), and (3) PLGA-PEG-PLGA (75/25) copolymers.

sphere. All the samples (Fig. 5a) show a variation of mass losses events, which are related to polymers decomposition process as a function of temperature. The mass losses are higher than 95% and the different mass losses are attributed to the different monomer ratios. With the increasing of LA content in PLGA, the decomposition temperature T_d decreases.

For the PLGA-PEG-PLGA (Fig. 5b), there are two steps of decomposition with T_d value around 280 and 340°C. The losses of PLGA occurred around 280°C and PEG at 340°C. As Khodaverdi [24] has reported that before increasing the temperature, the PLGA-PEG-PLGA copolymer system is a collosol for the hydrogen bonding between PEG segments and water molecules. With the temperature increasing, the hydrogen bonds become weaker, and hydrophobic bonds between PLGA chain segments begin to form hydrogel networks between the micelles. From the mass losses values of two decomposition steps, it is concluded that the PLGA and PEG segment ratios in

PLGA-PEG-PLGA are close to the expected theoretical values. This conclusion is in accordance with ^1H NMR results (Table 1). When the amount of PEG in PLGA-PEG-PLGA increased, the T_d value corresponding to PLGA decomposition also increased.

The degradation mechanism of PLGA is mainly about random hydrolytic chain scission. For the first step, the water absorption identified as a plasticizing compound made polymer chains more plastic and encouraged the reorganization of polymer segments [47, 48]. As GA content increased, both the rate and amount of water uptake increase, and on the contrary, lower water absorption and slower rate occur for the decrease of GA content in PLGA. Though PLGA degradation products have been well studied, the pathology of the sometimes observed bad biocompatibility is not clear. Daniels [49], Taylor [50] and coworkers have reported that local decrease in pH during degradation is the main reason for inflammatory response.

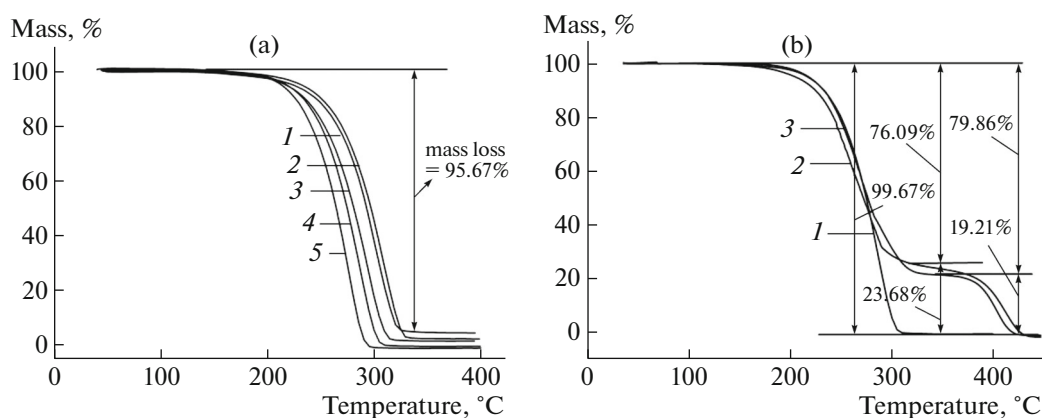


Fig. 5. TG curves of (a) PLGA polymers with different LA/GA ratios: (1) 50/50, (2) 60/40, (3) 70/30, (4) 80/20, (5) 90/10; (b) (1) PLGA (70/30), (2) PLGA-PEG-PLGA (50/50), and (3) PLGA-PEG-PLGA (75/25) copolymers.

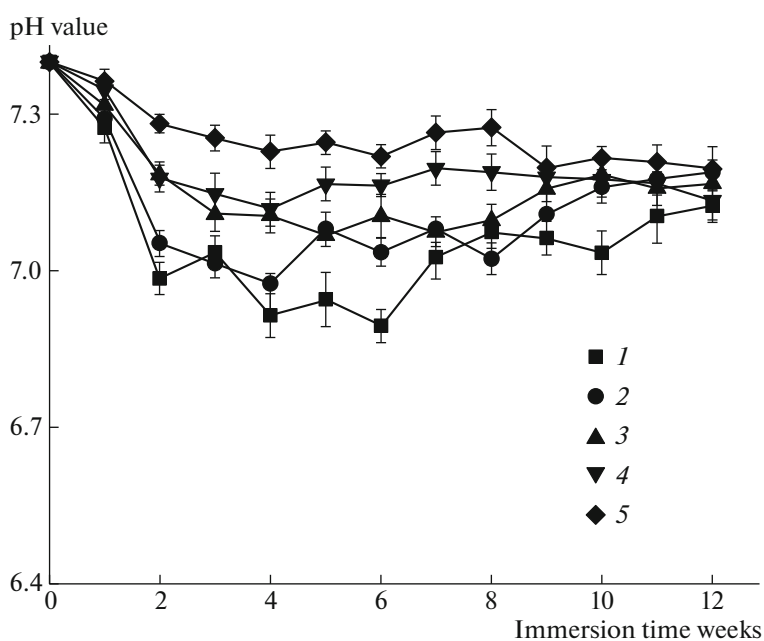


Fig. 6. In vitro degradation tests of different composition PLGA polymers: (1) 50/50, (2) 60/40, (3) 70/30, (4) 80/20, (5) 90/10. The results are given in degrees as a mean value \pm standard deviation ($n = 5$).

As PLGA showed a slower weight losses during the whole incubation time, its degradation behavior was monitored by measuring the changes of incubation buffer's pH values caused by the release of acidic oligomers from polymeric matrices. The in vitro degradation of PLGA was studied in PBS (pH 7.4) at 37°C, for 12 weeks in static conditions. PLGA degradation rate is mainly determined by the components of polymer chains. Altering the chemical composition such as raising the GA molar ratio will increase the degradation rate [51]. The PLGA (50/50) degrades most rapidly, whereas PLGA (90/10) is the most stable in these series (Fig. 6). According to these polymers' degradation curves, the incubation buffer's pH

remains stable for the first week. Nonetheless the pH for each PLGA decrease greatly at the next 2 weeks and then, stabilize around 5 weeks, a value lower than the initial pH (7.4) during all the incubation times. The pH reduction observed at initial three weeks is in agreement with the release of oligomers into the aqueous medium, formed during the preparation procedure, in the aqueous system.

Other studies have suggested the drug system degradation behaviors have a direct relationship with polymer concentrations [52]. So in order to keep a constant blood drug concentration, we can synthesize PLGA polymers with an appropriate degradation rate

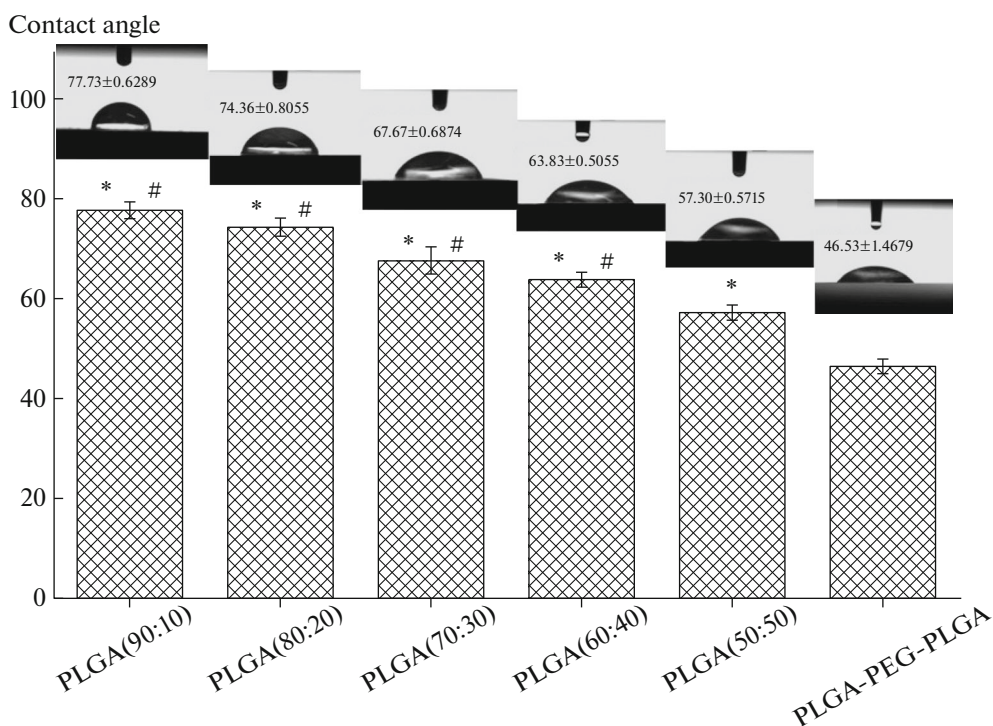


Fig. 7. Water contact angle measurements of different composition PLGA and PLGA-PEG-PLGA (75/25) copolymers. The results are given in degrees as a mean value \pm standard deviation ($n = 5$). *: Compared with PLGA-PEG-PLGA (75/25), $P < 0.05$. #: Compared with PLGA (50/50), $P < 0.05$.

which is in agreement with PLGA loaded drugs release rate.

The hydrophilicity of PLGA and PLGA-PEG-PLGA was determined by contact angle size [53]. Figure 7 shows that PLGA with different LA and GA ratios exhibit a wide range of hydrophilic properties. It is noticeable that the contact angle decrease gradually with increasing of GA content in polymer. PLGA (50/50) with a contact angle (57.3°) indicates better hydrophilicity compared to others PLGA polymers. Compared with PLGA (50/50), the triblock copolymer PLGA-PEG-PLGA (75/25) exhibits a better hydrophilicity due to the presence of PEG block.

The hydrophilic PLGA-PEG-PLGA copolymer will have better biocompatibility and it can deliver both hydrophobic and hydrophilic drugs. Moreover, the increasing of copolymer hydrophilicity can promote the stability of proteins and increase of the loading efficiency of water-soluble drugs and proteins as Deng reported [54]. In order to enhance the tissue and cell compatibility, the interfacial energy should be lessened by reducing material contact angle. Furthermore, the detached PEG surface layer induced by the tumor acidic microenvironment can facilitate cellular uptake, and the drugs were rapidly released within tumor cells due to the hydrophobic PLGA layer [30].

The cytotoxicity of PLGA (75/25) and PLGA-PEG-PLGA (75/25) copolymers were tested with

human U251 cells using MTT assay. MTT assay is used to determine the disruption of a critical biochemical function, which could quantify mitochondrial function by measuring the formation of dark blue formazan products. The MTT testing results are presented in Fig. 8. The relative percentage of control cells, which were not exposed to the transfection system, is used to represent 100% cell viability. As shown in graphs, for both these copolymers, cell survival rates are greater than 80%. With varying polymer concentrations treatments from 0.0625 to 4 mg/mL, none of the tested materials shows any significant cytotoxic effects on U251 cells making them suitable for biomedical applications. These data reveal that these copolymers are associated with a statistically high cell activity and both have the lowest cytotoxicity and highest cell compatibility at the concentration of 0.0625 mg/mL on days one.

PLGA polymers affect the metabolic activity of U251 cells during the incubation period of 24 h in a dose-dependent manner ranging from 0.0625 to 4 mg/mL. However, in comparison to PLGA, the cell viability remains slightly higher after incubated with PLGA-PEG-PLGA copolymers. One possible explanation for these little differences in cytotoxicity is different hydrophilic performance between two polymers lead to various cell adhesive ability. There is a significant difference in the toxicity of different formulations at almost each of the given concentrations ($P < 0.05$,

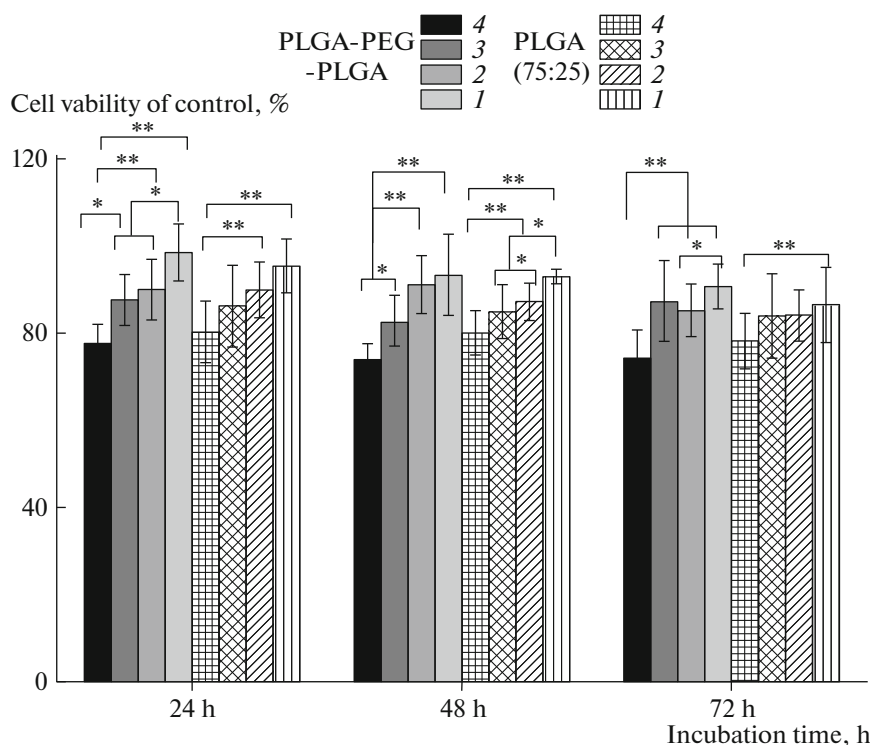


Fig. 8. Cell viability of PLGA (75/25) and PLGA-PEG-PLGA (75/25) copolymers after 24, 48, and 72 hours. Data represent means \pm standard deviation ($n = 5$). *: significant difference, $P < 0.05$, **: significant difference, $P < 0.01$. (1) 0.0625, (2) 0.25, (3) 1, and (4) 4 mg/mL.

$P < 0.01$). Cell viability slightly reduced at higher concentrations may be caused by the relatively higher concentrations of polymer degradation products. Therefore, it is conceivable that PLGA and PLGA-PEG-PLGA are generally accepted as being of low cytotoxicity with good biocompatibility, biodegradability and encouraged for future drug carrier without any significant cytotoxic effects.

CONCLUSIONS

In summary, a series of PLGA with different compositions and PLGA-PEG-PLGA were successfully prepared by modified ring-opening polymerization technique. The obtained results indicate that the ratios between the monomers in PLGA and PLGA-PEG-PLGA are very close to the expected theoretical values. The copolymer degradation behavior can be regulated by changing LA and GA monomer content. Hence, PLGA (70/30) with an appropriate degradation rate can keep a constant blood drug concentration. But likewise, the hydrophilicity, in vitro degradation and cytotoxicity tests indicated that PLGA-PEG-PLGA (75/25) copolymer has better hydrophilicity, biocompatibility and biodegradability, which could be a suitable vehicle for long-acting, controlled release delivery system. These results demonstrate that PLGA (75/25) and PLGA-PEG-

PLGA (75/25) are considered as promising carriers for the drugs delivery.

ACKNOWLEDGMENTS

This work was supported by the Hong Kong, Macao and Taiwan Science and Technology Cooperation Program of China (no. 2015DFH30180) and the Key Technology Research Project of Wuhan Municipality (no. 2014060202010120). We have also benefited from the National Natural Science Foundation of China (no. 51403168) and the Science and Technology Support of Hubei Province-Performance Evaluation of Public Technology Innovation Platform (no. 2015BCE022).

REFERENCES

1. C. D. Erbetta, R. J. Alves, J. M. Resende, R. F. Freitas, and R. G. Sousa, *J. Biomater. Nanobiotechnol.* **3**, 208 (2012).
2. S. B. Zhou, X. M. Deng, X. H. Li, W. X. Jia, and L. Liu, *J. Appl. Polym. Sci.* **91**, 1848(2004).
3. X. Zhu and R. D. Braatz, *J. Biomed. Mater. Res., Part A* **103A**, 2269 (2015).
4. C. I. A. van Houdt, R. S. Preethanath, and B. A. J. A. van Oirschot, *J. Biomed. Mater. Res., Part A* **104A**, 483 (2016).

5. Y. L. Haber, O. Pinkas, S. Boehm, T. Scheper, C. Kasper, and M. Machluf, *Biomed. Microdevices* **15**, 1055 (2013).
6. D.-H. Lee, T.-Y. Kwon, K.-H. Kim, S.-T. Kwon, D.-H. Cho, S. H. Jang, J. S. Son, and K.-B. Lee, *Polym. Bull.* **71**, 1933 (2014).
7. R. B. Shah and S. P. Schwendeman, *J. Controlled Release* **196**, 60 (2014).
8. S. D. Nath, S. Son, A. Sadiasa, Y. K. Min, and B. T. Lee, *Int. J. Pharm.* **196**, 60 (2014).
9. B. Baghaei, S. H. Jafari, H. A. Khonakdar, M. R. Saeb, U. Wagenknecht, and G. Heinrichd, *Int. J. Polym. Mater.* **64**, 641 (2015).
10. C. López-Santos, A. Terriza, J. Portolés, F. Yubero, and A. R. González-Elipe, *J. Phys. Chem. C* **119**, 20446 (2015).
11. A. Naik, S. M. Best, and R. E. Cameron, *Mater. Sci. Eng. C* **48**, 642 (2015).
12. X. S. Wu and N. Wang, *J. Biomater. Sci., Polym. Ed.* **12**, 21 (2001).
13. E. Vey, C. Rodger, L. Meehan, J. Booth, M. Claybourn, A. F. Miller, and A. Saiani, *Polym. Degrad. Stab.* **97**, 358 (2012).
14. C. R. Osswald and J. J. Kang-Miele, *Ann. Biomed. Eng.* **43**, 2609 (2015).
15. T. Jiang, R. R. Petersen, G. Call, G. Ofek, J. Gao, J. Q. Yao, *J. Biomed. Mater. Res., Part B* **97B**, 355 (2011).
16. J. K. Vasir and V. Labhasetwar, *Adv. Drug Deliv. Rev.* **59**, 718 (2007).
17. J. Meeus, D. J. Scurr, B. Appeltans, K. Amssoms, P. Annaert, M. C. Davies, C. J. Roberts, and G. V. Mooter, *Eur. J. Pharm. Biopharm.* **90**, 22 (2015).
18. Q. Fan, F. Qi, C. Miao, H. Yue, F. Gong, J. Wu, G. Ma, and Z. Su, *Colloids Surf., A* **500**, 177 (2016).
19. J. Di, J. Kim, Q. Hu, X. Jiang, and Z. Gu, *J. Controlled Release* **220**, 592 (2015).
20. X. Tang, Y. Liang, X. Feng, R. Zhan, X. Jin, and L. Sun, *Mater. Sci. Eng. C* **49**, 348 (2015).
21. Q. Yan, L. Q. Xiao, L. Tan, W. Sun, T. Wu, L. W. Chen, Y. Mei, and B. Shi, *J. Biomed. Mater. Res., Part A* **103A**, 3580 (2015).
22. L. Chen, X. Li, L. Cao, X. Li, J. Meng, J. Dong, L. Yua, and J. Ding, *Chin. J. Polym. Sci.* **34**, 147 (2016).
23. L. Zhang, W. Shen, J. Luan, D. Yang, G. Wei, L. Yu, W. Lu, and J. Ding, *Acta Biomater.* **23**, 271 (2015).
24. E. Khodaverdi, F. S. M. Tekie, F. Hadizadeh, H. Esmaeel, S. A. Mohajeri, S. A. S. Tabassi, and G. Zohuri, *AAPS PharmSciTech* **15**, 177 (2014).
25. L. Yu, G. T. Chang, H. Zhang, and J. D. Ding, *Int. J. Pharm.* **348**, 95 (2008).
26. S. Chen, R. Pieper, D. C. Webster, and J. Singh, *Int. J. Pharm.* **288**, 207 (2005).
27. X. Zhang, X. Zeng, X. Liang, Y. Yang, X. Li, H. Chen, L. Huang, L. Mei, and S. Feng, *Biomaterials* **35**, 9144 (2014).
28. B. Patel, V. Gupta, and F. Ahsan, *J. Controlled Release* **162**, 310 (2012).
29. Z. Song and G. Zhai, *J. Colloid Interface Sci.* **354**, 116 (2011).
30. C. Xu, H. Zhang, C. Sun, Y. Liu, S. Shen, X. Yang, Y. Zhu, and J. Wang, *Biomaterials* **88**, 48 (2016).
31. S. C. Yadav, A. Kumari, and R. Yadav, *Peptides* **32**, 173 (2011).
32. T. Simón-Yarza, F. R. Formiga, E. Tamayo, B. Pelacho, F. Prosper, and M. J. Blanco-Prieto, *Int. J. Pharm.* **440**, 13 (2013).
33. F. Yu, Y. Li, C. S. Liu, Q. Chen, G. H. Wang, W. Guo, X. E. Wu, D. H. Li, W. D. Wu, and X. D. Chen, *Int. J. Pharm.* **484**, 181 (2015).
34. Y. Gao and S. Gao, *J. Drug Targeting* **19**, 516 (2011).
35. N. Wang, X. S. Wu, C. Li, and M. F. Reng, *J. Biomater. Sci., Polym. Ed.* **11**, 301 (2000).
36. C. Ouyang, G. Ma, S. X. Zhao, L. Wang, L. P. Wu, Y. Wang, C. X. Song, and Z. P. Zhang, *Polym. Bull.* **67**, 793 (2011).
37. S. Davaran, A. Rezaei, S. Alimohammadi, A. A. Khandaghi, K. N. Koshki, H. T. Nasrabadi, and A. Akbarzadeh, *Adv. Nanopart.* **3**, 14 (2014).
38. J. Fagerland and A. Finne-Wistrand, *J. Polym. Res.* **21**, 337 (2014).
39. A. Ortín, M. J. Montesinos, E. López, P. Hierro, B. Monrabal, J. R. Lapasió, and C. García, *Macromol. Symp.* **330**, 6 (2013).
40. H. Fasehee, R. Dinarvand, A. Ghavamzadeh, M. E. Manesh, H. Moradian, S. Faghghi, and S. H. Ghaffri, *J. Nanobiotechnol.* **14**, 32 (2016).
41. M. Ionov, J. Lazniewska, V. Dzmitruk, I. Halets, S. Loznikova, D. Novopashina, E. Apartsin, O. Krasheninina, A. Venyaminova, K. Milowska, O. Nowacka, R. G. Ramirez, F. J. Mata, J. P. Majoral, D. Shcharbin, and M. Bryszewska, *Int. J. Pharm.* **485**, 261 (2015).
42. N. Yoneki, T. Takami, T. Ito, R. Anzai, K. Fukuda, K. Kinoshita, S. Sonotaki, and Y. Murakami, *Colloids Surf., A* **469**, 66 (2015).
43. F. R. Kang and J. Singh, *Int. J. Pharm.* **260**, 149 (2003).
44. Y. Duan, Y. Zhang, T. Gong, and Z. Zhang, *J. Mater. Sci.: Mater. Med.* **18**, 2067 (2007).
45. R. C. Mundargi, V. Rangaswamy, and T. M. Aminabhavi, *J. Appl. Polym. Sci.* **122**, 2244 (2011).
46. E. Saadat, A. Abdollahi, and F. A. Dorkoosh, *J. Pharm. Innovation* **10**, 118 (2015).
47. P. Blasi, S. S. D'Souza, F. Selmin, and P. P. DeLuca, *J. Controlled Release* **108**, 1 (2005).
48. R. Dorati, C. Colonna, M. Serra, I. Genta, T. Modena, and F. Pavanetto, *AAPS PharmSciTech* **9**, 718 (2008).
49. A. U. Daniels, M. S. Taylor, K. P. Andriano, and J. Heller, *Proc. Orthop. Res. Soc.* **88**, 260 (1992).
50. M. S. Taylor, A. U. Daniels, K. P. Andriano, and J. Heller, *J. Appl. Biomater.* **5**, 151 (1994).
51. R. Dorati, C. Colonna, I. Genta, T. Modena, and B. Conti, *Polym. Degrad. Stab.* **95**, 694 (2010).
52. J. K. Perron, H. E. Naguib, J. Daka, A. Chawla, and R. Wilkins, *J. Biomed. Mater. Res., Part B* **91**, 876 (2009).
53. M. Sampath, R. Lakra, P. Korrapati, and B. Sengottuvelan, *Colloids Surf., B* **117**, 128 (2014).
54. X. M. Deng, C. D. Xiong, L. M. Cheng, H. H. Huang, and R. P. Xu, *J. Appl. Polym. Sci.* **55**, 1193 (1995).